Published in final edited form as:

J Immunol. 2018 August 01; 201(3): 861–873. doi:10.4049/jimmunol.1701717.

Anti-insulin B cells are poised for antigen presentation in type 1 diabetes[2]

Jamie L. Felton[*], **Damian Maseda**[†], **Rachel H. Bonami**[‡], **Chrys Hulbert**[‡], **James W. Thomas**[†,‡]

[*] Department of Pediatrics, Division of Pediatric Endocrinology, Vanderbilt University Medical Center

[†] Department of Pathology, Microbiology and Immunology, Vanderbilt University

[‡] Department of Medicine, Division of Rheumatology and Immunology, Vanderbilt University

Abstract

Early breaches in B cell tolerance are central to type 1 diabetes progression in mouse and man. Conventional BCR transgenic mouse models (VH125.Tg NOD) reveal the power of B cell specificity to drive disease as APCs. However, in conventional, fixed-IgM models, comprehensive assessment of B cell development is limited. In order to provide more accurate insight into the developmental and functional fates of anti-insulin B cells, we generated a new NOD model (V_H125^{SD}.NOD) in which anti-insulin VDJH125 is targeted to the IgH chain locus to generate a small (1–2%) population of class switch-competent insulin-binding B cells. Tracking of this rare population in a polyclonal repertoire reveals that anti-insulin B cells are preferentially skewed into marginal zone and late transitional subsets known to have increased sensitivity to pro-inflammatory signals. Additionally, IL-10 production, characteristic of regulatory B cell subsets, is increased. In contrast to conventional models, class switch-competent anti-insulin B cells proliferate normally in response mitogenic stimuli but remain functionally silent for insulin autoantibody production. Diabetes development is accelerated, which demonstrates the power of anti-insulin B cells to exacerbate disease without differentiation into antibody-forming or plasma cells. Autoreactive T cell responses in V_H125^{SD}.NOD mice are not restricted to insulin autoantigens, as evidenced by increased IFN-γ production to a broad array of diabetes-associated epitopes. Together, these results independently validate the pathogenic role of anti-insulin B cells in T1D, underscore their diverse developmental fates, and demonstrate the pathologic potential of coupling a critical beta cell specificity to predominantly pro-inflammatory antigen presenting B cell subsets.

Keywords

B cells; transgenic mice; autoimmunity; diabetes; anergy

[2]Abreviations used: B6, C57BL/6; FO, follicular; MFI, mean fluorescence intensity; MZ, marginal zone; PLN, pancreatic lymph node; pre-MZ, pre-marginal zone; SFC, spot forming cell; T1, transitional 1; T1D, type 1 diabetes; T2, transitional 2; Tg, transgene

Address correspondence to Dr. James Thomas, Vanderbilt University, Medical Center North T-3113, 1161 21st Avenue South, Nashville, TN 37232. james.w.thomas@vanderbilt.edu. Fax: 615-322-6248.

Introduction

Type 1 diabetes (T1D) results from the autoimmune destruction of insulin producing beta cells, leading to chronic hyperglycemia and a lifelong need for exogenous insulin. In humans, T1D is predicted by the emergence of autoantibodies to insulin and other islet antigens before the onset of clinical symptoms (1); thus, an early breach in B cell tolerance is central to disease development. Despite the large body of literature emphasizing the predictive power of autoantibodies for progression to clinical T1D (reviewed in ref. 2), relatively little is known about the autoreactive B cells that produce them. While autoantibodies alone cannot induce beta cell destruction (3), autoreactive B cells are not benign. In addition to antibody production, B cells function as potent, diabetogenic APCs (4, 5). Evidence of their pathogenic potential was revealed when B cell deficient NOD mice were found to be protected from diabetes (6–9). In new onset T1D patients, selective depletion of B cells with an anti-CD20 monoclonal antibody (Rituximab) temporarily improved beta cell function (10). As the critical role that B cells play in driving T1D is increasingly recognized, understanding the relationship between the functional state of B cells and breaches in B cell tolerance is essential for identifying early targets for disease prevention and reversal.

Autoreactive B cells comprise up to 75% of the immature B cell repertoire (11). In non-autoimmune environments, autoreactive B cells that evade central tolerance and escape into the periphery are maintained in an anergic state, characterized by developmental arrest, impaired proliferation to B cell mitogens, and functional silencing for autoantibody production (12). In autoimmune conditions, this anergic state is often compromised, and autoimmunity results from the failure of autoreactive cells to maintain their unresponsiveness (13, 14). The study of rare B cell populations has been revolutionized by the development of Ig transgenic mouse models that permit the tracking of autoreactive B cells that are below the level of detection in physiologic conditions (13). In the anti-dsDNA transgenic mouse model for systemic lupus erythematous, anti-dsDNA B cells are developmentally arrested in BALB/c mice; however, in the autoimmune-prone MRL strain, B cells overcome both developmental arrest and follicular exclusion to become antibody-producing B cells (14). To assess the functional state of autoreactive B cells in T1D, our group previously developed an insulin-specific, conventional transgenic mouse model (VH125.Tg), in which an insulin-specific heavy chain was introduced into the germline of NOD mice as an IgM^a transgene (Tg). In these mice, a small population of insulin-binding B cells support the development of T1D, while mice harboring the same Tg without insulin binding do not (15, 16). When paired with anti-insulin Vk-125, insulin-binding B cells enter mature subsets and upregulate co-stimulatory molecules but are anergic to B cell mitogens and fail to produce autoantibodies. These data on a conventional IgM-only Tg model suggest the importance of anti-insulin B cells in the development of T1D and further indicate that functionally anergic anti-insulin B cells may support disease (5, 16, 17).

However, the conventional VH125.Tg model is limited by several factors. The Tg copy number and the integration site in the genome are not known and therefore remain variables that have the power to affect disease development in the conventional model. Further, the IgM-only Tg is not competent to class switch, which limits the precise staging of B cell

development. Further, in the absence of class switch recombination, it is impossible to assess the production of IgG autoantibodies, which are currently the most accurate predictors of T1D development in genetically susceptible individuals (18–20). To address how a fully functional, anti-insulin VH gene impacts disease, we targeted VDJH125 to the IgH chain locus in embryonic stem cells and used them to produce C57BL/6 (B6) and NOD mice harboring an anti-insulin VH (V_H125^{SD}) (21, 22).

In non-autoimmune prone B6 mice, these autoreactive B cells do not generate insulin autoantibodies spontaneously or in response to T-dependent immunization with heterologous insulin, and they have impaired proliferation to anti-CD40 and insulin in vitro. However, tolerance can be reversed following combined BCR/TLR stimulation which results in antigen-specific germinal center responses and antibody production (21). Whether tolerance is similarly maintained in an autoimmune environment, however, is unknown. Therefore, we assessed the phenotype, development, and functional capacity of these autoreactive B cells in transgenic NOD mice (V_H125^{SD}.NOD). We found that site-directed anti-insulin B cells on the NOD background develop into mature B cell subsets that are enriched at the late transitional (T2) and marginal zone (MZ) stages and proliferate in response to B cell mitogens. The enriched T2 population in the spleen is also detected at the site of attack in pancreatic lymph nodes (PLNs), providing a reservoir of B cells that are primed to become MZ-like anti-insulin B cells. Their capacity to proliferate following mitogenic stimulation reflects the unique responsiveness of T2 B cells to innate and environmental stimuli (23). Also consistent with this T2 predominance is the increased IL-10 production by anti-insulin B cells in V_H125^{SD}.NOD mice (24). However, anti-insulin antibody responses, both spontaneous autoantibody production and T-dependent antibody responses following immunization, remain impaired. Even in this state, V_H125^{SD}.NOD mice develop more intense insulitis and accelerated diabetes development compared to their non-transgenic littermates. Although the B cell repertoire is skewed toward insulin, T cell responses in V_H125^{SD}.NOD mice maintain diverse specificities for multiple beta cell autoepitopes.

Importantly, this model independently validates the pathogenic role of anti-insulin B cells in T1D that was demonstrated in previous, conventional IgM transgenic models, and confirms the capacity of anti-insulin B cells to accelerate the rate of T1D development without an overt loss of tolerance and differentiation to produce autoantibodies. These studies also highlight the multiple, developmental fates of anti-insulin B cells in the periphery, including subsets sensitive to pro-inflammatory signals, in addition to subsets with regulatory potential, as evidenced by increased anti-insulin B cell IL-10 production. Thus, potential opportunities for B cell directed therapy in T1D include limiting innate environmental cues that expand pro-inflammatory subsets as well as facilitating expansion of regulatory B cells.

Methods

Animals

NOD mice were originally procured from Taconic Biosciences, Inc. Anti-insulin VDJ_H-125 from our original H+L chain 125Tg (25) mice was cloned to generate a targeting vector, pIV_H-SAH-125-VDJ_H (21). Founder mice were generated by targeting 129Ola embryonic stem cells and then backcrossed to NOD for at least 10 generations. Southern blot was used

to confirm the presence of the targeted allele. All mice were housed under specific pathogen-free conditions, and all studies were approved by the institutional use and animal care committee of Vanderbilt University Medical Center, fully accredited by the AAALAC. Both male and female mice were used to characterize B cell development and function while female mice were employed in disease studies.

Cell isolation, flow cytometry, and antibodies

Single cell suspensions from spleen and PLNs were prepared using HBSS (Invitrogen Life Technologies) + 10% FBS (HyClone). Spleen RBCs were lysed using Tris-NH_4Cl. Cells were subsequently stained for flow cytometry analysis in 1X PBS containing 0.1% sodium azide, 0.02% EDTA, and 1% FBS using the following reagents and reactive antibodies (BD Biosciences or eBiosciences): Fixable Viability Stain 700 for cell viability, B220 (6B2), CD19 (1D3), CD21 (7G6), CD23 (B3B4), IgM (15F9), IgD (11–26c), IgM^a (DS-1), IL-21 (mhalx21) and IL-10 (JES5–16E3, BioLegend). Insulin-binding BCRs were detected using biotinylated human insulin (Sigma-Aldrich) (26). Insulin-occupied BCRs were detected using biotinylated anti-insulin mAb123 (ATCC #HB-123) (27). The insulin epitope recognized by mAb123 is distinct from the mAb125 insulin epitope used to derive V_H125.Tg. mAb123 detects anti-insulin V_H125^{SD}.NOD BCR occupancy with endogenous insulin, but not insulin bound to the insulin receptor (25, 28). Avidin-fluorochrome conjugates (BD Biosciences) were used to detect biotinylated reagents. Samples were acquired using a BD Biosciences LSR II flow cytometer, and FlowJo software (Tree Star, Inc) was used for data analysis.

Cytokine Analysis

Lymphocytes from the spleens and PLNs of V_H125^{SD}.NOD mice were cultured in 96-well plates in the presence or absence of plate-bound anti-CD3ε (145–2C11, BD Biosciences) and soluble anti-CD28 (37.51, BD Biosciences) stimulation. Stimulated wells were coated with anti-CD3ε and washed with PBS prior to adding media and cells. All cells were cultured in cell culture media (RPMI 1640 [Cellgro] containing 10% FBS, 1% L-glutamine, 1% HEPES, 0.2% gentamicin, and 0.1% 2-ME; Life Technologies). For stimulated wells, 1μg/ml anti-CD28 (clone 37.51; BD Pharmingen) in cell culture media was added. For unstimulated wells, media alone was added. Cells were cultured at 38°C at 5% CO_2 for 60h. Intracellular cytokine staining for IL-21 (mhalx21, eBioscience) was performed using BD Cytofix/Cytoperm™ solutions (BD Pharmingen) according to manufacturer's instructions after stimulation for 4h with PMA (50ng/ml; Sigma), ionomycin (500ng/ml; Sigma), and monensin (2μM; eBioscience). Intracellular cytokine staining for IL-10 (JES5–16E3, BioLegend) was performed using BD Cytofix/Cytoperm™ solutions (BD Pharmingen) after stimulation for 4h with PMA, ionomycin, LPS, and monesin as previously described (29).

Proliferation Assays

Proliferation of B cells was measured by dye dilution assays. Splenocytes were isolated and re-suspended in pre-warmed cell culture media (RPMI 1640 [Cellgro] containing 10% FBS, 1% L-glutamine, 1% HEPES, 0.2% gentamicin, and 0.1% 2-ME; Life Technologies). Cells were stained with CellTrace™ Violet (CTV) dye (Invitrogen) per manufacturer's instructions (5mM stock solution of CTV was prepared by adding 20μL of DMSO), and 1μL

of CTV was added per 1×10^6 cells. Labeled cells were incubated with LPS, anti-IgM (AffiniPure F(ab')2 Fragment Goat Anti-Mouse IgM, μ chain specific; Jackson ImmunoResearch Laboratories, Inc), or anti-CD40 (HM40–3; BD Biosciences) with and without IL-4 and incubated at 37°C in 5% CO_2 for 3.5 days. After incubation, cells were stained for flow cytometry as described above. Data was analyzed and proliferation index calculations were made with FlowJo software (Tree Star, Inc).

Immunization

Pre-immune sera were collected from male, pre-diabetic NOD or V_H125^{SD}.NOD mice between 8 and 12 weeks of age. Mice were immunized subcutaneously at the base of the tail with insulin peptide B:10–23 (10μg/0.1ml, Schafer-N) emulsified in CFA. Sera were harvested 2 weeks following immunization.

Detection of antibodies by ELISA

Ninety-six well maxisorp Nunc plates (Thermoscientific) were coated with 1μg/mL of human insulin in borate-buffered saline overnight at 37°C. Sera diluted 1:100 in 1X PBS was added and plates were incubated overnight at 4°C. Parallel samples were co-incubated with 100μg/mL human insulin to inhibit specific binding. Antibodies were detected with goat anti-mouse IgG conjugated to alkaline phosphatase (Southern Biotech, 1030–04) incubated 1h at room temperature. Plates were washed with 0.05% TWEEN 20 in 1X PBS after each incubation step. 10mg/mL *p*-nitrophenyl phosphate substrate (Sigma-Aldrich) was added and OD was read at 405nm using a Microplate Autoreader (Bio-Tek Instruments). Anti-insulin mAb123 (HB-123, ATCC) was purified from hybridoma supernatant and used to generate standard curves for quantification of spontaneous anti-insulin IgG production. Specific insulin antibody binding was calculated by subtracting the OD detected in the presence of 10X insulin as an inhibitor.

Insulitis and diabetes incidence assessment

Insulitis assessment and disease studies were performed using female mice. Pancreata were dissected from non-diabetic mice and fixed with neutral buffered formalin for 4–6h and then incubated overnight in 70% ethanol at room temperature. Tissues were embedded in paraffin, 5μm sections were cut, and slides were stained with H&E by the Vanderbilt Translational Pathology Shared Resource Core. Slide images were acquired using a bright field Aperio ScanScope CS (Leica Biosystems). Aperio ImageScope software (Leica Biosystems) was used to blind score images for insulitis according to the following scale: 0 = no insulitis; 1 = < 25% lymphocytic infiltration; 2 = 25–50% lymphocytic infiltration; 3 = 50–75% lymphocytic infiltration; 4 = > 75% lymphocytic infiltration. All islets in a section were scored (average = 28 per section, min = 9, max = 51) and the percentages of islets with each score were averaged across all mice in the cohort to eliminate bias from differences in the number of islets counted per mouse. Blood glucose was measured weekly in mice beginning at 10 weeks of age. Mice were considered diabetic after the first of two consecutive readings > 200 mg/dL.

Detection of T cell responses by ELISpot

IFN-γ producing cells were assessed via ELISpot for evaluation of pro-inflammatory T cell responses (30–32). Ninety-six well filter plates (Millipore) were incubated for 5 minutes in room temperature 70% ethanol. After washing plates with sterile 1X PBS, they were coated with 100μl of 0.5μg/ml anti-mouse IFN-γ capture antibody (R4–6A2) diluted in sterile 1X PBS and incubated overnight at 4°C. Blocking solution (RPMI 1640 [Cellgro] containing 10% FBS, 1% L-glutamine, 1% HEPES, 0.2% gentamicin, and 0.1% 2-ME; Life Technologies) was added to wells and incubated for 2h at room temperature in the dark to block non-specific membrane binding. Splenocytes were harvested from non-transgenic NOD and V_H125^{SD}.NOD female pre-diabetic mice between 10 and 14 weeks of age. HBSS (Invitrogen Life Technologies) + 10% FBS (HyClone) was used to macerate spleens and RBCs were lysed using Tris-NH_4Cl. Splenocytes were plated at 1×10^6 cells/well in 100μl plus 100μl of RPMI (control) or 100μl of 10μM peptide antigen (Schafer-N). Plates were incubated at 37°C in 5% CO_2 for 72h. After incubation, cell suspension was discarded and plates were washed with deionized water, followed by wash buffer (1X PBS/0.05% TWEEN 20). Plate was coated with biotinylated anti-mouse IFN-γ detection antibody (R4–6A2) and incubated at room temperature in the dark for 2h. HSP-streptavidin antibody was added prior to an additional 1h incubation at room temperature. Plates were washed with wash buffer followed by 1X PBS. AEC substrate set (BD Biosciences) was used per manufacturer's instructions for plate development. Cold deionized water was used to stop the reaction, and dry plates were read on an ImmunoSpot plate reader (Cellular Technology Limited). Data are expressed as the average of technical triplicates of the number of spot forming cells (SFCs) per well.

Statistical analysis

Statistical analyses were performed using GraphPad Prism 7.0a for MacOS (GraphPad Software, La Jolla, CA, USA). Throughout, asterisks are used to denote *p*-values by indicated statistical test: * $p < 0.05$, ** $p < 0.01$, *** $p < 0.001$.

Results

V_H125^{SD}.NOD mice generate anti-insulin B cells that encounter endogenous insulin

Previous studies used a fixed IgM transgene to investigate anti-insulin B cells in T1D prone NOD mice (16, 17, 33, 34). To assess the fate and function of more physiologic, class switch-competent, anti-insulin B cells, NOD mice that harbor anti-insulin VDJ_H-125 site-directed to the IgH chain locus were developed as described in Williams et al. (21) and Methods. Flow cytometry on splenocytes was used to track the targeted allele (a allotype) and revealed that for V_H125^{SD}.NOD mice, allelic exclusion was effective with >90% of all B cells staining positive for IgM^a (Figure 1B). IgM^a pairs with endogenous V-kappa chains to generate a small population of anti-insulin B cells (2.1 ± 0.3%, n=14; Fig. 1A, left panel). The binding specificity is confirmed by competitive inhibition with excess, unlabeled insulin (21). These findings contrast non-transgenic NOD mice (Fig. 1A, right panel) in which insulin-binding is rare (<0.1%) and binding is not specifically inhibited by excess insulin (16).

To determine whether anti-insulin BCRs encounter insulin at physiologic insulin levels in vivo, a biotinylated, anti-insulin monoclonal antibody (mAb123) was used to detect insulin-occupied BCRs (17, 25, 27, 33). B cells were harvested from V_H125^{SD}.NOD mice and stained either immediately with biotinylated mAb123, or after being loaded with human insulin, washed, and then stained with biotinylated mAb123 as a positive control and to assess maximal BCR occupancy (Fig. 1C). Both the percent of insulin-binding B cells and the mean fluorescence intensity (MFI) of mAb123+ B cells (indicative of occupied BCRs) were lower compared to values using insulin-loaded B cells. These findings are consistent with previous observations that anti-insulin BCRs are occupied by endogenous insulin in V_H125^{SD}.B6 mice (21) and NOD mice that express the conventional H and L anti-insulin Tg (125Tg) (25) and indicate that under physiologic conditions, where insulin circulates at low concentrations (1ng/ml), anti-insulin BCRs in V_H125^{SD}.NOD mice encounter endogenous insulin but may not be fully occupied.

Immature anti-insulin B cells that leave the bone marrow successfully undergo peripheral maturation

Immature B cells that leave the bone marrow complete their development in the periphery to become FO or MZ B cells (35). To investigate peripheral B cell maturation in V_H125^{SD}.NOD mice, flow cytometry on lymphocytes was used to identify insulin-binding and non-insulin binding B cells, and IgM and IgD expression was tracked. Insulin-binding B cells were compared to non-insulin-binding B cells in the spleen and PLNs of V_H125^{SD}.NOD mice. The representative flow plots in Fig. 1D reveal both $IgM^{a\ high}$ and $IgM^a/D^{a\ high}$ B cells in the spleen, and primarily $IgM^a/D^{a\ high}$ B cells in the PLNs. The increased percentage of $IgM^{a\ high}/IgD^{a\ low}$ B cells in the spleen (28.9±3.5%, n = 3) compared to the PLNs (2.0±0.4%, n=3) is consistent with previous studies demonstrating increased numbers of MZ splenic B cells in NOD mice (Fig. 1E) (36, 37).

To further interrogate the developmental fate of fully functional, class switch-competent B cells in V_H125^{SD}.NOD mice, flow cytometry was used to identify B cell subsets. T1 ($CD21^{low}$ $CD23^{low}$ IgM^{high}), T2 ($CD21^{low}$ $CD23^{high}$ IgM^{high}), FO ($CD21^{low}$ $CD23^{high}$ IgM^{low}), pre-MZ ($CD21^{high}$ $CD23^{high}$ IgM^{high}) and MZ ($CD21^{high}$ $CD23^{low}$ IgM^{high}) subsets were detected in both autoreactive insulin-binding and non-insulin-binding B cells (Fig. 1F). Overall, frequencies of insulin-binding and non-insulin-binding B cells were not different in T1 or pre-MZ stages (Fig. 1G). Significantly increased frequencies of T2 and MZ B cells were observed in the insulin-binding B cells compared to non-insulin-binding B cells ($p < 0.001$ for each subset). While anti-insulin B cells can enter all peripheral B cell compartments, they are enriched in the T2 and MZ subsets which are recognized for their heightened responsiveness to innate signals and enhanced capacity for antigen presentation (23, 38–40). Conversely, the frequencies of FO B cells were significantly decreased in the insulin-binding population compared to non-insulin-binding B cells ($p < 0.001$). This is in striking contrast to the developmental fate of site-directed insulin-binding B cells in a non-autoimmune environment, in which anti-insulin B cells in V_H125^{SD}.B6 mice predominantly occupy the FO subset with only a small percentage (2.5%) of anti-insulin B cells developing into MZ B cells (21). Together, these results demonstrate that anti-insulin B cells derived

from a single transgene in V_H125^{SD}.NOD successfully develop into functionally heterogeneous mature B cells, characterized by predominant T2 and MZ compartments.

Distinct insulin-binding B cells populate the spleen and PLNs in V_H125^{SD}.NOD mice

We next sought to determine whether insulin-binding B cells were characterized by a distinct developmental fate in V_H125^{SD}.NOD mice. Because the incidence of diabetes development is known to be higher in female compared to male NOD mice (41), we examined B cell subsets from both genders. When V_H125^{SD}.NOD anti-insulin B cells are identified by flow cytometry, distinct populations emerge in the spleen in both male and female mice and can be distinguished by differential insulin binding and IgM expression (Fig. 2A, E). Similar distinct populations are identified in the PLNs, the initial site of interaction between islet autoantigens and autoreactive lymphocytes (Fig. 2C, G). Given the developmental and functional heterogeneity of anti-insulin B cells, we sought to determine whether distinct populations of anti-insulin B cells tracked with different developmental fates. Anti-insulin B cells identified in V_H125^{SD}.NOD spleen and PLNs were divided into two groups based on their intensity of insulin binding: “low MFI” and “high MFI,” and each group was interrogated for developmental phenotypes by flow cytometry (Fig. 2B, D, F, H). In the spleen and PLNs of both male and female mice, the percentage of “low MFI” anti-insulin B cells in the late transitional (T2 subset) was significantly lower than the percentage of “high MFI” anti-insulin B cells ($p<0.001$ for female spleen and male PLN cells, $p<0.01$ for male spleen cells, $p<0.05$ for female PLN cells) (2I). In the FO subset, there was a significantly increased percentage of “low MFI” populations compared to “high MFI” populations in for all groups ($p<0.001$ for female spleen and male PLN cells, $p<0.01$ for male spleen cells, $p<0.05$ for female PLN cells). While the overall percentages of anti-insulin B cells that distributed into the T1 subset were universally <10%, a statistically significant increase in the percentage of T1 cells that were “low MFI” compared to “high MFI” was observed in the female and male spleen cells ($p<0.05$ and $p<0.001$), but not in the PLNs. For all groups, “high MFI” anti-insulin B cells reside primarily in primarily T2 subsets, while “low MFI” anti-insulin B cells distributed between the T2 and FO subsets. Though not statistically different between “high MFI” and “low MFI” populations, small but identifiable populations of MZ cells were noted in the PLNs in both female and male mice (Fig. 2I). The qualitative similarity in B cell subsets of insulin-binding cells in male and female NOD mice are consistent with previously published observations reporting similar islet lymphocyte subset distribution in male and female mice (42). These results show that in V_H125^{SD}.NOD mice, anti-insulin B cells have the capacity to enter all mature subsets but are enriched in the MZ subset compared to non-insulin-binding B cells (Fig. 1G). Anti-insulin B cells with higher insulin affinity (“high MFI”) are enriched in T2 subsets in the spleen and PLNs, yet only lower affinity (“low MFI”) anti-insulin B cells developed into FO subsets, indicating that BCR affinity for self-antigen influences anti-insulin B cell developmental fate.

Late transitional (T2) B cells have been shown to correspond to regulatory, IL-10 producing B cell subsets in autoimmune disease models (24). In NOD mice, IL-10+ B cells diminished inflammatory T cell responses to islet-associated peptides ex vivo (43). Given the T2 predominance observed in insulin-binding B cells with high insulin affinity, we interrogated

these cells for IL-10 production via intracellular cytokine staining. CD19+IL-10+ cells expressed higher surface levels of MHC-II and CD1d (44) antigen presenting molecules compared to their CD19+IL-10- counterparts. Surprisingly, they also exhibited high levels of insulin binding (Fig. 3A, B). Interrogating the IL-10 production capacity within different CD1d and insulin-binding subsets revealed a 5-fold increase in CD19+CD1d− insulin-binding cells and a >20-fold increase in CD19+CD1d++ insulin-binding cells relative to the CD19+CD1d− non-insulin-binding lymphocyte subset. Thus, while anti-insulin B cells are favorably selected into subsets known to sense inflammatory signals (23), these subsets also include B cells with the potential for immune regulation.

Anti-insulin B cells in V_H125^{SD}.NOD are not anergic to mitogens

Previous studies used H + L chain anti-insulin BCRs from NOD and B6 mice to show that anti-insulin B cells were anergic (5, 21). In these studies, H + L chain insulin specificity was required to enable adequate cell numbers for assessment of proliferation via thymidine incorporation assay. To directly assess the functional capacity of the small, naturally occurring anti-insulin B cell population in V_H125^{SD}.NOD mice, we used flow cytometry and CellTrace™ Violet labeling to investigate proliferative responses to B cell mitogens. To ensure that the capacity to proliferate was not affected by the transgene itself, proliferative responses for all B cells from non-transgenic NOD and V_H125^{SD}.NOD mice were first compared. Splenic B cells were cultured with B cell mitogens LPS, anti-IgM, or anti-CD40, and proliferation was tracked. The percentage of divided cells was used to quantify and compare proliferative responses. There was no significant difference in proliferative responses for non-transgenic NOD B cells compared to V_H125^{SD}.NOD B cells ($p = 0.5$) (Supp. Fig. 1A). We then gated on insulin-binding and non-insulin-binding V_H125^{SD}.NOD B cells and compared responses to determine whether insulin-binding affected proliferation. A dose response was quantified to determine optimal stimulation concentration for each mitogen (Fig. 4A). After culture with mitogen, B cell proliferation was quantified by measuring the percentage of dividing cells and determining the proliferation index. Proliferative responses were observed for both non-insulin-binding and insulin-binding B cells for each stimulus. A representative dot plot and histogram in Fig. 4B reveal that proliferation for anti-insulin B cells was comparable to proliferation for non-insulin-binding B cells. Further, no differences between the percentage of dividing cells or the proliferation index were detected (Fig. 4C). As expected, CD86 expression was upregulated in both non-insulin-binding and insulin-binding B cells following stimulation (Supp. Fig. 1B). Therefore, targeted anti-insulin B cells in V_H125^{SD}.NOD mice are not anergic to optimal stimulation by B cell mitogens, unlike the conventional H + L anti-insulin transgenic B cells in previous models. Further, these responses are consistent with the unique T2 predominance that characterizes V_H125^{SD}.NOD anti-insulin B cells, as T2 B cells have been shown to exhibit heightened responsiveness to mitogenic stimulation (23).

Antibody production is impaired in V_H125^{SD}.NOD anti-insulin B cells

To determine whether V_H125^{SD}.NOD B cells remained functionally silent for antibody production, insulin antibody was assessed in non-transgenic male NOD and V_H125^{SD}.NOD mice before and after immunization with the immunodominant B:9–23 insulin peptide in CFA (45). Anti-insulin serum IgG was measured prior to and two weeks following

immunization. While non-transgenic NOD mice mounted a significant increase in antibody production 2 weeks after immunization (mean OD_{405} 0.158, $p < 0.05$), V_H125^{SD}.NOD mice did not (Fig. 5A). Spontaneous autoantibody production prior to immunization was also reduced in V_H125^{SD}.NOD mice compared to non-transgenic controls. Some, albeit reduced, antibody production was observed in a proportion of V_H125^{SD}.NOD mice (mean OD_{405} 0.019). When these low levels of antibody were interrogated for allotype and IgG isotype, we found that IgG anti-insulin antibodies produced by V_H125^{SD}.NOD mice were universally “b” allotype. Thus, small populations of endogenous B cells, and not transgenic anti-insulin B cells, are responsible for low level antibody production in V_H125^{SD}.NOD mice (Fig. 5B). The IgG2a isotype predominated responses by both transgenic and non-transgenic NOD mice, which is consistent with previous observations (46). Together these findings indicate that anti-insulin B cells in V_H125^{SD}.NOD mice are functionally silenced for undergoing differentiation into antibody producing cells in response to T-dependent immunization.

Insulitis and diabetes onset is accelerated in V_H125^{SD}.NOD mice

Previous studies show that a conventional IgM anti-insulin VH transgene supported T1D development in NOD mice and suggested a role for anti-insulin B cells in T1D (16). To determine how the same anti-insulin VH expressed from its physiologic locus impacts diabetes development, cohorts of female V_H125^{SD}.NOD mice and their non-transgenic NOD age-matched controls were assessed for insulitis, hyperglycemia, and spontaneous insulin autoantibody production ($n \geq 5$ mice per group). Insulitis was assessed histologically and was quantified based on the percentage of islet infiltration as described in Methods. In V_H125^{SD}.NOD mice, greater percentages of islets were infiltrated throughout disease progression (assessed at 8–12 weeks, 13–16 weeks, and 17–20 weeks) compared to non-transgenic NOD age-matched controls (Fig. 6A). Further, insulitis scores, which quantified the extent of islet infiltration, were consistently higher in V_H125^{SD}.NOD mice compared to non-transgenic NOD mice and were significantly higher in the 13–16 week cohort ($p< 0.01$) (Fig. 5B). To determine whether spontaneous autoantibody production could be detected over time, anti-insulin serum IgG was measured for each cohort. In non-transgenic NOD mice, spontaneous antibody production was observed as early as 8 weeks and increased between 13 and 20 weeks (Fig. 6C, black diamonds). In V_H125^{SD}.NOD mice, no spontaneous antibody production was detected prior to 17 weeks. After 17 weeks, anti-insulin IgG was identified in some mice, but its production was overall blunted compared to non-transgenic NOD mice, despite the increased frequency of insulin-binding B cells (Fig. 6C, white diamonds).

Diabetes development was assessed in cohorts of female V_H125^{SD}.NOD mice and their non-transgenic littermates (n=13 for each group) through weekly monitoring for hyperglycemia. Compared to non-transgenic littermates, V_H125^{SD}.NOD mice develop diabetes at an accelerated rate. Average age of disease onset did not differ between groups (12 weeks). However, by 17 weeks, over 50% of V_H125^{SD}.NOD mice had developed diabetes, while over 50% of their non-transgenic littermates remained disease free until 27 weeks. By 33 weeks, disease penetrance was 100% for V_H125^{SD}.NOD mice, compared to only 54% for non-transgenic littermates (Fig. 6D). These results are consistent with our previously

published disease studies in conventional (fixed-IgM) V_H125Tg.NOD mice compared to non-transgenic (wild-type) NOD littermates (16, 17, 34). The outcomes in these previous cohorts are compared to the current study in Fig 6E. In order to compare cohorts of mice studied at different times and from different suppliers, we determined the age at which the incidence of diabetes first exceeded 50% (I-50%) in transgenic NOD mice and littermate controls. In all cohorts, disease is shown to be accelerated by 9–10 weeks in mice that harbor anti-insulin transgenes, either conventional or targeted. In contrast, when we determined the age of diabetes onset each cohort, the absolute difference in the mean age of onset for all disease studies ranged from 0–2 weeks. Thus, onset of diabetes is not increased in mice harboring anti-insulin VH transgenes; however, disease progression is markedly accelerated when an anti-insulin transgene is present (Fig. 6E). Together, these data further support the observation that B cell specificity has the power to alter disease progression and that increased frequencies of insulin-specific B cells will accelerate disease development, despite functional silencing of autoantibody production.

T cell responses to a broad array of epitopes are increased in V_H125^{SD}.NOD mice

Given the imperative role that B cells play as APCs in diabetes development (5, 47), we sought to determine whether the disease acceleration observed in V_H125^{SD}.NOD mice was the result of skewing the T cell repertoire toward anti-insulin pathological responses. IFN-γ production was assessed for a broad array of autoepitopes, including insulin, proinsulin and non-insulin epitopes recognized as autoantigens in T1D, including mouse proinsulin-1 (PI 15–23; SPGDLQTLALEVARQKRG), mouse proinsulin-2 (PI 19–31; LELGGGPGAGDLQTLALEVA), mouse GAD 524–543 (GADp35; SRLSKVAPVIKARMMEYGTT), mouse GAD 217–236 (GADp15; EYVTLKKMREIIGWPGGSGD) (32), a chromogranin A derived epitope ChgA 342–355 (WE14; WSKMDQLAKELTAE) (35), and a recently identified fusion peptide (HIP; LQTLAL-WSRMD) (48). We used an anti-MHC-II antibody to confirm that the majority of IFN-γ production observed was the result of CD4 T cell-B cell interaction upon antigen presentation. In the presence of anti-MHC-II antibody, the percentage of IFN-γ producing cells was reduced by 91.0±3.1% and 78.2±4.7% in non-transgenic NOD and V_H125^{SD}.NOD mice, respectively (data not shown). Responses were not restricted to insulin, rather they included multiple non-insulin epitopes. A clear trend toward increased responses to insulin epitopes as well as multiple, non-insulin epitopes was observed in V_H125^{SD}.NOD mice (Fig. 7A). Given the heterogeneous nature of diabetes progression in mice and man, the variability of inflammatory responses was anticipated. To determine whether similar trends towards increased IFN-γ responses persisted when variability was minimized, we cultured splenocytes from age-matched V_H125^{SD}.NOD and their non-transgenic NOD littermates in the presence or absence of insulin and the immunodominant B chain epitope (B:10–23, HLVEALYLVCGERG), and IFN-γ production was assessed. In V_H125^{SD}.NOD mice, there was a trend towards increased IFN-γ production at baseline (in the absence of antigen) and after culture with insulin and B:10–23, compared to non-transgenic NOD littermates, and a statistically significant increase IFN-γ production in response to insulin compared to no stimulation in V_H125^{SD}.NOD mice ($p<0.05$) was revealed in V_H125^{SD}.NOD splenocytes, specifically (Fig. 7B). An increased frequency of B cells favoring insulin-binding in V_H125^{SD}.NOD mice supports a breach in tolerance to multiple beta cell autoantigens and is

consistent with studies suggesting that insulin is an important early and/or primary target in T1D (49).

In addition to IFN-γ, IL-21 production was also assessed to more fully interrogate the inflammatory T cell responses in V_H125^{SD}.NOD mice, as IL-21 has been shown to be requisite for disease development and correlate with disease severity (50, 51). Because we were unable to assess antigen-specific IL-21 responses, intracellular cytokine staining was used to detect IL-21 production by transgenic and non-transgenic NOD mice in response to anti-CD3 and anti-CD28 stimulation. CD4 T cells in the spleen of V_H125^{SD}.NOD mice produced IL-21 in response to mitogenic stimulation (Supp. Fig. 2A) which was not different than IL-21 production by non-transgenic NOD mice (Supp. Fig. 2B). IL-21 production in response to mitogenic stimulation was detected in both the spleen and PLNs of V_H125^{SD}.NOD and non-transgenic NOD mice. While there was a statistically significant increase in IL-21 production before and after stimulation in the spleen and PLNs of V_H125^{SD}.NOD mice, there was no significant difference between IL-21 MFI in transgenic compared to non-transgenic mice either at baseline or after stimulation (Supp. Fig. 2C).

Discussion

Here we describe an anti-insulin BCR transgenic NOD mouse model (V_H125^{SD}.NOD) in which anti-insulin VDJH125 is targeted to the IgH chain locus and recombines with endogenous V kappa chains to generate functional BCRs. This single copy VH transgene generates a small population (1–2%) of class switch-competent, insulin-binding B cells and accelerates the development of insulitis and diabetes in the NOD mouse. Previous studies in a co-adoptive transfer model show that these anti-insulin B cells interact with TCR transgenic T cells that recognize a diabetogenic epitope (22). In this study, we examine the development and function of anti-insulin B cells in the natural, polyclonal repertoire of NOD mice. BCRs in V_H125^{SD}.NOD mice provide more accurate insight into the developmental status and functional state of anti-insulin B cells in the context of autoimmune diabetes. While anti-insulin B cells have multiple fates, we find a majority are preferentially skewed into T2 and MZ-like subsets that have increased sensitivity to pro-inflammatory and innate signals (23, 52). Consistent with this heightened sensitivity to innate signals, anti-insulin B cells in V_H125^{SD}.NOD mice proliferate normally in response to B cell mitogens. This finding in a polyclonal repertoire differs from the anergic state observed in anti-insulin B cells from monoclonal (H+L chain) repertoires (5, 21, 25) and may explain why disease progression in NOD mice that harbor anergic H+L chain anti-insulin BCRs is less aggressive (16, 36). T cell responses in V_H125^{SD}.NOD mice are not focused on insulin epitopes, as demonstrated by increased CD4 T cell responses to a broad array of diabetes-associated antigens, including GAD epitopes and a recently identified hybrid insulin peptide (48). Together, these studies suggest that the developmental skewing of anti-insulin B cells into T2 and MZ-like subsets may foster their antigen-presenting functions and connect innate signals with adaptive autoimmunity.

Autoreactive B cell development is influenced by a multitude of factors, including, but not limited to, the quantity of circulating antigen and its interaction with BCRs (53, 54). By using a second anti-insulin monoclonal antibody to detect endogenous rodent insulin on

BCRs in V_H125^{SD}.NOD mice, we verify that autoreactive B cell development is not simply the result of clonal ignorance. Rather, our data confirms and extends the concept that, despite its low levels, insulin in circulation is sufficient to engage anti-insulin BCRs and affect anti-insulin B cell fate. Studies on BCR occupancy indicate that not all potential insulin-binding BCRs are engaged, a finding that reflects the dynamic nature of circulating insulin levels required to maintain glucose homeostasis. This observation highlights the importance of physiologic models of tolerance compared to transgene expression of foreign proteins (13, 55–57). Previous work by our group shows that different insulin-binding populations are characterized by two predominant L chains (5, 17, 40). In V_H125^{SD}.NOD mice, distinct insulin-binding populations can also be visualized. In addition to the populations detected in the conventional VH125Tg, the targeted transgene reveals a population of insulin-binding B cells in which IgM is down-regulated, and this hallmark of tolerance (57) is observed in the spleen and at the site of autoimmune attack in PLNs. Therefore, functional diversity arises in anti-insulin B cells that emerge in V_H125^{SD}.NOD mice as a consequence of differences in BCR affinity and variable encounters with the hormone in circulation.

Intact class switch recombination in the V_H125^{SD}.NOD model permits more precise tracking of anti-insulin B cell developmental fate as characterized by differential IgM and IgD expression. In NOD mice, the MZ subset ($IgM^{high}IgD^{low}$) is recognized to be increased at the expense of FO ($IgD^{high}IgM^{low}$) B cells (39). In V_H125^{SD}.NOD mice, anti-insulin B cells track predominantly to the T2 subset ($IgM^{high}IgD^{high}$) and these cells are observed in both the spleen and draining PLNs. Some anti-insulin B cells also enter mature MZ and FO subsets. In contrast to non-insulin binding B cells, the frequency of MZ anti-insulin B cells exceeds that of FO anti-insulin B cells in V_H125^{SD}.NOD mice. Thus, the fate of anti-insulin B cells in NOD mice differs appreciably from anti-insulin B cells in V_H125^{SD}.B6 mice and other murine models of disease in non-autoimmune (C57BL/6) backgrounds, such as B cells that express the *Ptpn22* autoimmune risk variant (58), which are characterized by a FO subset predominance (21). Therefore, while anti-insulin B cells are competent to enter both MZ and FO subsets, the balance of their developmental fate is governed by the genetic environment. MZ-like B cells have been shown to colonize extrasplenic locations in female NOD mice, including PLNs and pancreas where they are considered to act as potent APCs for diabetogenic T cells (52). We also identify small numbers of MZ-like B cells ($CD21^{high}CD23^{low}$) in PLNs of V_H125^{SD}.NOD mice. As the late transitional T2 subset is recognized to be uniquely sensitive to innate environmental signals with the potential to expand into antigen-specific MZ B cells (23), we propose that T2 B cells in V_H125^{SD}.NOD mice are poised to become MZ-like B cells at the site of autoimmune attack. Recent elegant studies demonstrate that islet macrophages in NOD mice display an increased inflammatory signature that is associated with early T1D (59). Our findings suggest that the heightened sensitivity of T2 and MZ anti-insulin B cells to these same innate signals further enhance the pathogenic microenvironment in V_H125^{SD}.NOD mice.

Additional phenotypic diversity in anti-insulin B cells is observed in our finding of an increase in IL-10 producing anti-insulin B cells compared to non-insulin binding B cells in the same mice. Thus, despite their overall detrimental influence on T1D, some anti-insulin B cells with regulatory potential remain in the repertoire. Regulatory B cells with T2 and pre-

MZ phenotypes have been identified in models of autoimmune disease and have regulatory effects via IL-10 production (24). Interestingly, signals that rely on innate receptors TLR4 and TLR9 are also capable of IL-10 regulatory B cell expansion (60). However, IL-10 production in V_H125^{SD}.NOD mice does not appear to exert meaningful disease suppression. A possible explanation for this apparent paradox is that anti-inflammatory properties of IL-10 may be influenced by site of exposure, as demonstrated by the acceleration of diabetes in NOD mice with islet-specific IL-10 expression compared to prevention of diabetes with systemic IL-10 treatment (61). Future studies evaluating the production of IL-10 by anti-insulin B cells in the PLNs and islets in V_H125^{SD}.NOD mice are needed to more fully understand the relationship between B cells, IL-10, and disease progression in the NOD mouse.

Using an approach that differs from previous models, assessment anti-insulin B cell function in V_H125^{SD}.NOD mice reveals that anti-insulin B cell mitogen responses remain intact in a polyclonal repertoire. In IgM-restricted H+L chain BCR transgenic mouse models, tolerance has been characterized by anergy to stimulation through the BCR (anti-IgM), TLR4 (LPS), and CD40 (anti-CD40) (36). Unexpectedly, V_H125^{SD}.NOD anti-insulin B cells, generated with the same V_H125 transgene used in conventional models, are not anergic to stimulation with B cell mitogens. We used CellTrace™ Violet and flow cytometry-based tracking to evaluate rare, insulin-binding populations in a polyclonal repertoire to show that the large majority of insulin-binding B cells undergo cell division in response to a panel of conventional B cells mitogens. These data are consistent with the recognized responsiveness of T2 B cells to stimulation by innate signals, and this may extend to the site of autoimmune attack (23, 38, 59).

Insulin autoantibodies are strong predictors of T1D development in humans and in mice (62). In particular, IgG insulin autoantibodies (IAA) have been associated with aggressive disease progression. However, prior to the development of V_H125^{SD}.NOD mice, IgG autoantibodies for insulin could not be assessed because conventional transgenic mouse models are unable to class switch. Class switch-competent V_H125^{SD}.NOD mice develop accelerated diabetes, but insulin autoantibody production is significantly impaired. When low levels of IgG anti-insulin antibodies are detected following immunization, they originate from endogenous (b allotype) rather than transgenic B cells. Thus, anti-insulin B cells harboring VDJH125 are functionally silenced for autoantibody production in the polyclonal repertoire of V_H125^{SD}.NOD mice. However, in a co-adoptive transfer model, anti-insulin TCR transgenic T cells are able to reverse the tolerant state of V_H125^{SD}.NOD anti-insulin B cells, resulting in germinal center and antibody production (22). Together, these results suggest that antibody production by anti-insulin B cells in V_H125^{SD}.NOD mice requires a critical threshold of T cell help, and that functional silencing for antibody production is reversed when T cell help is increased using TCR transgenic T cells.

This threshold may be achieved incrementally. Initially, innate signals may enhance antigen presentation by T2 and MZ-like anti-insulin B cells that capture antigen and present key autoepitopes, such as B:9–23, to rare pathogenic T cells. As pathogenic T cells expand they may interact with and reverse tolerance of silent anti-insulin B cells, or they may encounter naïve anti-insulin B cells and drive their differentiation in germinal center reactions. In this

way, IgG autoantibodies to insulin provide a barometer for generation of autoreactive T cells and evidence that cognate T-B cell interactions capable of driving disease have occurred.

IFN-γ has proved a useful cytokine for identifying correlates of T1D exacerbation in NOD mice (30–32). Using this response as a metric of autoreactivity, we show that V_H125^{SD}.NOD mice have significantly increased spontaneous IFN-γ production by CD4 T cells and increased production of IFN-γ to a broad array of beta cell autoantigens, in addition to insulin. However, the role of IFN-γ in NOD mice is complex and incompletely understood, encompassing potentially protective tolerogenic as well as diabetogenic effects (63). Among T cell subsets, T follicular helper cells (Tfh) are the most dependent on B lymphocytes for their development and function (64). Several studies suggest that Tfh cells play an important role in mouse and human T1D (65–67) and IL-21, the principal cytokine produced by Tfh cells, is shown to be critical for disease progression in NOD mice (50, 51). Approaches to assess antigen specific induction of IL-21 are not available, but we do find that both V_H125^{SD}.NOD and non-transgenic, wild type NOD mice produce comparable IL-21 responses following polyclonal stimulation. Although IL-21 production was not different between transgenic and non-transgenic NOD mice, Th1 and IL-21-producing Tfh cells are known to share molecular regulators, including T-bet and Bcl6 (68); therefore, increased differentiation of IFN-γ producing T cells in V_H125^{SD}.NOD mice is expected to provide a reservoir for the generation of IL-21-secreting Tfh cells. Understanding how insulin-specific B cells impact the Tfh cell compartment is an important area for future investigation.

These studies provide several important caveats that are relevant to therapeutic interventions in T1D. Small increases in unfavorable B cell specificities in the repertoire have a large effect on the rate of T1D progression, at least in part by enhancing autoantigen/epitope spread. Thus, removal of limited pernicious specificities from the repertoire may delay or prevent disease without the risks associated with total B cell depletion (10). Targeting of autoantigen binding V regions by anti-idiotypes (69) or other serologic agents (70) could accomplish this goal. However, current studies tend to focus on specificities identified for circulating autoantibodies; our findings suggest that these specificities may reflect the interactions that occur late in the autoimmune process when the autoreactive T cell population is well expanded. Identifying critical early B cell specificities rather than circulating antibodies may uncover more accurate targets. Emerging technologies for capturing and expanding rare B cells are well suited for achieving this goal (71). Critical B cell specificities, such as our anti-insulin V_H125^{SD}, reside in B cell subsets that are programmed to respond to innate signals; therefore, modifications to the innate environment could alter their response potential. For example, gut microbiota are recognized to alter T1D outcomes (72, 73), and their innate signals may be expected to modify the responses of T2/MZ-like B cells. Further, not all anti-insulin B cells are pathogenic. Rare anti-insulin B cells that produce IL-10 are clearly present and could be expanded so that their regulatory potential can be favorably exploited. Studies on the role of B cells in T1D beyond autoantibody production have been limited. Our findings tracking B cells that recognize one key beta cell autoantigen, insulin, illustrate the potential importance of B cells in understanding the pathogenesis of T1D and identify new approaches for disease intervention.

Supplementary Material

Refer to Web version on PubMed Central for supplementary material.

Acknowledgments

This work was supported by the NIH grant R01 AI051448, NICHD grant 5T32HD060554-06A1, CTSA award No. UL1TR000445 from the National Center for Advancing Translational Sciences, and funding from the Endocrine Fellows Foundation. This work was also supported through the Vanderbilt Translational Pathology Shared Resource (supported by NIH grants 5U24 DK059637) and the Vanderbilt Medical Center Flow Cytometry Shared Resource (supported by the Vanderbilt Ingram Cancer Center [P30 CA68485]). Its contents are solely the responsibility of the authors and do not necessarily represent official views of the National Center for Advancing Translational Sciences or the National Institutes of Health.

References

1. Ziegler AG, Rewers M, Simell O, Simell T, Lempainen J, Steck A, Winkler C, Ilonen J, Veijola R, Knip M, Bonifacio E, and Eisenbarth GS 2013 Seroconversion to multiple islet autoantibodies and risk of progression to diabetes in children. J. Am. Med. Assoc 309: 2473–2479.
2. Watkins RA, Evans-Molina C, Blum JS, and Dimeglio LA 2014 Established and emerging biomarkers for the prediction of type 1 diabetes: A systematic review. Transl. Res 164: 110–121. [PubMed: 24662515]
3. Petersen JS, Marshall MO, Baekkeskov S, Hejnaes KR, Høier-Madsen M, and Dyrberg T 1993 Transfer of type 1 (insulin-dependent) diabetes mellitus associated autoimmunity to mice with severe combined immunodeficiency (SCID). Diabetologia 36: 510–515. [PubMed: 8335172]
4. Jaume JC, Parry SL, Madec A-M, Sønderstrup G, and Baekkeskov S 2002 Suppressive effect of glutamic acid decarboxylase 65-specific autoimmune B lymphocytes on processing of T cell determinants located within the antibody epitope. J. Immunol 169: 665–672. [PubMed: 12097368]
5. Kendall PL, Case JB, Sullivan AM, Holderness JS, Wells KS, Liu E, and Thomas JW 2013 Tolerant anti-insulin B cells are effective APCs. J. Immunol 190: 2519–2526. [PubMed: 23396943]
6. Serreze DV, Chapman HD, Varnum DS, Hanson MS, Reifsnyder PC, Richard SD, Fleming SA, Leiter EH, and Shultz LD 1996 B lymphocytes are essential for the initiation of T cell-mediated autoimmune diabetes: analysis of a new “speed congenic” stock of NOD.Ig mu null mice. J. Exp. Med 184: 2049–2053. [PubMed: 8920894]
7. Noorchashm H, Noorchashm N, Kern J, Rostami SY, Barker CF, and Naji A 1997 B-cells are required for the initiation of insulitis and sialitis in nonobese diabetic mice. Diabetes 46: 941–946. [PubMed: 9166663]
8. Akashi T, Nagafuchi S, Anzai K, Kondo S, Kitamura D, Wakana S, Ono J, Kikuchi M, Niho Y, and Watanabe T 1997 Direct evidence for the contribution of B cells to the progression of insulitis and the development of diabetes in non-obese diabetic mice. Int. Immunol 9: 1159–1164. [PubMed: 9263013]
9. Wong FS, Visintin I, Wen L, Granata J, Flavell R, and Janeway CA 1998 The role of lymphocyte subsets in accelerated diabetes in nonobese diabetic-rat insulin promoter-B7–1 (NOD-RIP-B7–1) mice. J. Exp. Med 187: 1985–1993. [PubMed: 9625758]
10. Pescovitz MD, Greenbaum CJ, Krause-Steinrauf H, Becker DJ, Gitelman SE, Goland R, Gottlieb PA, Marks JB, McGee PF, Moran AM, Raskin P, Rodriguez H, Schatz DA, Wherrett D, Wilson DM, Lachin JM, and Skyler JS 2009 Rituximab, B-Lymphocyte Depletion, and Preservation of Beta-Cell Function. N. Engl. J. Med 361: 2143–2152. [PubMed: 19940299]
11. Wardemann H, Yurasov S, Schaefer A, Young JW, Meffre E, and Nussenzweig MC 2003 Predominant autoantibody production by early human B cell precursors. Science 301: 1374–1377. [PubMed: 12920303]
12. Glynne R, Akkaraju S, Healy JI, Rayner J, Goodnow CC, and Mack DH 2000 How self-tolerance and the immunosuppressive drug FK506 prevent B-cell mitogenesis. Nature 403: 672–676. [PubMed: 10688206]

13. Cambier JC, Gauld SB, Merrell KT, and Vilen BJ 2007 B-cell anergy: From transgenic models to naturally occurring anergic B cells? Nat. Rev. Immunol 7: 633–643. [PubMed: 17641666]
14. Mandik-Nayak L, Seo SJ, Sokol C, Potts KM, Bui A, and Erikson J 1999 MRL-lpr/lpr mice exhibit a defect in maintaining developmental arrest and follicular exclusion of anti-double-stranded DNA B cells. J Exp Med 189: 1799–1814. [PubMed: 10359584]
15. Zhang L, Nakayama M, and Eisenbarth GS 2008 Insulin as an autoantigen in NOD/human diabetes. Curr. Opin. Immunol 20: 111–118. [PubMed: 18178393]
16. Hulbert C, Riseili B, Rojas M, and Thomas JW 2001 Cutting Edge: B Cell Specificity Contributes to the Outcome of Diabetes in Nonobese Diabetic Mice. J. Immunol 167: 5535–5538. [PubMed: 11698422]
17. Henry RA, Kendall PL, and Thomas JW 2012 Autoantigen-specific B-cell depletion overcomes failed immune tolerance in type 1 diabetes. Diabetes 61: 2037–2044. [PubMed: 22698916]
18. Achenbach P, Bonifacio E, and Ziegler A-G 2005 Predicting type 1 diabetes. Curr. Diab. Rep 5: 98–103. [PubMed: 15794911]
19. Bonifacio E, and Ziegler AG 2010 Advances in the prediction and natural history of type 1 diabetes. Endocrinol. Metab. Clin. North Am 39: 513–525. [PubMed: 20723817]
20. Achenbach P, Koczwara K, Knopff A, Naserke H, Ziegler AG, and Bonifacio E 2004 Mature high-affinity immune responses to (pro)insulin anticipate the autoimmune cascade that leads to type 1 diabetes. J. Clin. Invest 114: 589–597. [PubMed: 15314696]
21. Williams JM, Bonami RH, Hulbert C, and Thomas JW 2015 Reversing Tolerance in Isotype Switch–Competent Anti-Insulin B Lymphocytes. J. Immunol 195: 853–864. [PubMed: 26109644]
22. Wan X, Thomas JW, and Unanue ER 2016 Class-switched anti-insulin antibodies originate from unconventional antigen presentation in multiple lymphoid sites. J. Exp. Med 213: 967–978. [PubMed: 27139492]
23. Meyer-Bahlburg A, Andrews SF, Yu KOAA, Porcelli SA, and Rawlings DJ 2008 Characterization of a late transitional B cell population highly sensitive to BAFF-mediated homeostatic proliferation. J. Exp. Med 205: 155–168. [PubMed: 18180309]
24. Evans JG, Chavez-Rueda KA, Eddaoudi A, Meyer-Bahlburg A, Rawlings DJ, Ehrenstein MR, and Mauri C 2007 Novel Suppressive Function of Transitional 2 B Cells in Experimental Arthritis. J. Immunol 178: 7868–7878. [PubMed: 17548625]
25. Rojas M, Hulbert C, and Thomas JW 2001 Anergy and not Clonal Ignorance Determines the Fate of B Cells that Recognize a Physiological Autoantigen. J. Immunol 166: 3194–3200. [PubMed: 11207272]
26. Bonami RH, Sullivan AM, Case JB, Steinberg HE, Hoek KL, Khan WN, and Kendall PL 2014 Bruton's Tyrosine Kinase Promotes Persistence of Mature Anti-Insulin B Cells. J. Immunol 192: 1459–1470. [PubMed: 24453243]
27. Thomas JW, Virta VJ, and Nell LJ 1986 Idiotypic determinants on human anti-insulin antibodies are cyclically expressed. J. Immunol 137: 1610–1615. [PubMed: 2427576]
28. Taylor SI, Schroer JA, and Marcus-Samuels B 1984 Binding of insulin to its receptor impairs recognition by monoclonal anti-insulin antibodies. Diabetes 33: 778–784. [PubMed: 6378700]
29. Maseda D, Smith SH, DiLillo DJ, Bryant JM, Candando KM, Weaver CT, and Tedder TF 2012 Regulatory B10 Cells Differentiate into Antibody-Secreting Cells After Transient IL-10 Production In Vivo. J. Immunol 188: 1036–1048. [PubMed: 22198952]
30. Arif S, Tree TI, Astill TP, Tremble JM, Bishop AJ, Dayan CM, Roep BO, and Peakman M 2004 Autoreactive T cell responses show proinflammatory polarization in diabetes but a regulatory phenotype in health. J. Clin. Invest 113: 451–463. [PubMed: 14755342]
31. Schloot NC, Hanifi-Moghaddam P, Goebel C, V Shatavi S, Flohé S, Kolb H, and Rothe H 2002 Serum IFN-gamma and IL-10 levels are associated with disease progression in non-obese diabetic mice. Diabetes. Metab. Res. Rev 18: 64–70. [PubMed: 11921420]
32. Kaufman DL, Tisch R, Sarvetnick N, Chatenoud L, Harrison LC, Haskins K, Quinn A, Sercarz E, Singh B, Von Herrath M, Wegmann D, Wen L, and Zekzer D 2001 Report from the 1st International NOD Mouse T-Cell Workshop and the Follow-Up Mini-Workshop. Diabetes 50: 2459–2463. [PubMed: 11679422]

33. Henry-Bonami RA, Williams JM, Rachakonda AB, Karamali M, Kendall PL, and Thomas JW 2013 B lymphocyte “original sin” in the bone marrow enhances islet autoreactivity in type 1 diabetes-prone nonobese diabetic mice. J. Immunol 190: 5992–6003. [PubMed: 23677466]
34. Kendall PL, Moore DJ, Hulbert C, Hoek KL, Khan WN, and Thomas JW 2009 Reduced diabetes in btk-deficient nonobese diabetic mice and restoration of diabetes with provision of an anti-insulin IgH chain transgene. J. Immunol 183: 6403–6412. [PubMed: 19841184]
35. Stadinski BD, Delong T, Reisdorph N, Reisdorph R, Powell RL, Armstrong M, Piganelli JD, Barbour G, Bradley B, Crawford F, Marrack P, Mahata SK, Kappler JW, and Haskins K 2010 Chromogranin A is an autoantigen in type 1 diabetes. Nat. Immunol 11: 225–231. [PubMed: 20139986]
36. Acevedo-Suárez C. a, Hulbert C, Woodward EJ, and Thomas JW 2005 Uncoupling of anergy from developmental arrest in anti-insulin B cells supports the development of autoimmune diabetes. J. Immunol 174: 827–833. [PubMed: 15634904]
37. Quinn WJ, Noorchashm N, Crowley JE, Reed AJ, Noorchashm H, Naji A, and Cancro MP 2006 Cutting Edge: Impaired Transitional B Cell Production and Selection in the Nonobese Diabetic Mouse. J. Immunol 176: 7159–7164. [PubMed: 16751358]
38. Petro JB, Gerstein RM, Lowe J, Carter RS, Shinners N, and Khan WN 2002 Transitional type 1 and 2 B lymphocyte subsets are differentially responsive to antigen receptor signaling. J. Biol. Chem 277: 48009–48019. [PubMed: 12356763]
39. Stolp J, Marino E, Batten M, Sierro F, Cox SL, Grey ST, and Silveira PA 2013 Intrinsic Molecular Factors Cause Aberrant Expansion of the Splenic Marginal Zone B Cell Population in Nonobese Diabetic Mice. J. Immunol 191: 97–109. [PubMed: 23740954]
40. Case JB, Bonami RH, Nyhoff LE, Steinberg HE, Sullivan AM, and Kendall PL 2015 Bruton’s Tyrosine Kinase Synergizes with Notch2 To Govern Marginal Zone B Cells in Nonobese Diabetic Mice. J. Immunol 195: 61–70. [PubMed: 26034172]
41. Hawkins TA, Gala RR, and Dunbar JC 1994 Prolactin modulates the incidence of diabetes in Male and female nod mice. Autoimmunity 18: 155–162. [PubMed: 7858100]
42. Young EF, Hess PR, Arnold LW, Tisch R, and Frelinger JA 2009 Islet lymphocyte subsets in male and female NOD mice are qualitatively similar but quantitatively distinct. Autoimmunity 42: 678–691. [PubMed: 19886740]
43. Kleffel S, Vergani A, Tezza S, Ben Nasr M, Niewczas MA, Wong S, Bassi R, D’Addio F, Schatton T, Abdi R, Atkinson M, Sayegh MH, Wen L, Wasserfall CH, O’Connor KC, and Fiorina P 2015 Interleukin-10+regulatory b cells arise within antigen-experienced CD40+B cells to maintain tolerance to islet autoantigens. Diabetes 64: 158–171. [PubMed: 25187361]
44. Amu S, Saunders SP, Kronenberg M, Mangan NE, Atzberger A, and Fallon PG 2010 Regulatory B cells prevent and reverse allergic airway inflammation via FoxP3-positive T regulatory cells in a murine model. J. Allergy Clin. Immunol 125: 1114–1124. [PubMed: 20304473]
45. Daniel D, Gill RG, Schloot N, and Wegmann D 1995 Epitope specificity, cytokine production profile and diabetogenic activity of insulin-specific T cell clones isolated from NOD mice. Eur. J. Immunol 25: 1056–1062. [PubMed: 7537670]
46. Thomas JW, Kendall PL, and Mitchell HG 2002 The natural autoantibody repertoire of nonobese diabetic mice is highly active. J. Immunol 169: 6617–6624. [PubMed: 12444175]
47. Noorchashm H, Lieu YK, Noorchashm N, Rostami SY, a Greeley S, Schlachterman A, Song HK, Noto LE, Jevnikar M, Barker CF, and Naji A 1999 I-Ag7-mediated antigen presentation by B lymphocytes is critical in overcoming a checkpoint in T cell tolerance to islet beta cells of nonobese diabetic mice. J. Immunol 163: 743–750. [PubMed: 10395666]
48. Delong T, Wiles TA, Baker RL, Bradley B, Barbour G, Reisdorph R, Armstrong M, Powell RL, Reisdorph N, Kumar N, Elso CM, DeNicola M, Bottino R, Powers AC, Harlan DM, Kent SC, Mannering SI, and Haskins K 2016 Pathogenic CD4 T cells in type 1 diabetes recognize epitopes formed by peptide fusion. Science 351: 711–714. [PubMed: 26912858]
49. Nakayama M, Abiru N, Moriyama H, Babaya N, Liu E, Miao D, Yu L, Wegmann DR, Hutton JC, Elliott JF, and Eisenbarth GS 2005 Prime role for an insulin epitope in the development of type 1 diabetes in NOD mice. Nature 435: 220–223. [PubMed: 15889095]

50. Sutherland APR, Van Belle T, Wurster AL, Suto A, Michaud M, Zhang D, Grusby MJ, and Von Herrath M 2009 Interleukin-21 is required for the development of type 1 diabetes in nod mice. Diabetes 58: 1144–1155. [PubMed: 19208913]
51. McGuire HM, Walters S, Vogelzang A, Lee CMY, Webster KE, Sprent J, Christ D, Grey S, and King C 2011 Interleukin-21 is critically required in autoimmune and allogeneic responses to islet tissue in murine models. Diabetes 60: 867–875. [PubMed: 21357471]
52. Mariño E, Batten M, Groom J, Walters S, Liuwantara D, Mackay F, and Grey ST 2008 Marginal-zone B-cells of nonobese diabetic mice expand with diabetes onset, invade the pancreatic lymph nodes, and present autoantigen to diabetogenic T-cells. Diabetes 57: 395–404. [PubMed: 18025414]
53. Gaudin E, Hao Y, Rosado MM, Chaby R, Girard R, and Freitas AA 2004 Positive Selection of B Cells Expressing Low Densities of Self-reactive BCRs. J. Exp. Med 199: 843–853. [PubMed: 15024048]
54. Goodnow CC 1996 Balancing immunity and tolerance: deleting and tuning lymphocyte repertoires. Proc. Natl. Acad. Sci 93: 2264–2271. [PubMed: 8637861]
55. Goodnow CC 1992 Transgenic mice and analysis of B-cell tolerance. Annu. Rev. Immunol 10: 489–518. [PubMed: 1590994]
56. Nemazee D, Russell D, Arnold B, Hahmmerling G, Allison J, Miller JFAP, Morahan G, and Buerki K 1991 Clonal Deletion of Autospecific B Lymphocytes. Immunol. Rev 122: 117–132. [PubMed: 1937539]
57. Goodnow CC, Crosbie J, Jorgensen H, Brink RA, and Basten A 1989 Induction of self-tolerance in mature peripheral B lymphocytes. Nature 342: 385–391. [PubMed: 2586609]
58. Metzler G, Dai X, Thouvenel CD, Khim S, Habib T, Buckner JH, and Rawlings DJ 2017 The Autoimmune Risk Variant PTPN22 C1858T Alters B Cell Tolerance at Discrete Checkpoints and Differentially Shapes the Naive Repertoire. J. Immunol 199: 2249–2260. [PubMed: 28801357]
59. Ferris ST, Zakharov PN, Wan X, Calderon B, Artyomov MN, Unanue ER, and Carrero JA 2017 The islet-resident macrophage is in an inflammatory state and senses microbial products in blood. J. Exp. Med 214: 2369–2385. [PubMed: 28630088]
60. Tedder TF 2015 B10 Cells: A Functionally Defined Regulatory B Cell Subset. J. Immunol 194: 1395–1401. [PubMed: 25663677]
61. Balasa B, La Cava A, Van Gunst K, Mocnik L, Balakrishna D, Nguyen N, Tucker L, and Sarvetnick N 2000 A Mechanism for IL-10-Mediated Diabetes in the Nonobese Diabetic (NOD) Mouse: ICAM-1 Deficiency Blocks Accelerated Diabetes. J. Immunol 165: 7330–7337. [PubMed: 11120869]
62. Zhang L, and Eisenbarth GS 2011 Prediction and prevention of Type 1 diabetes mellitus. J. Diabetes 3: 48–57. [PubMed: 21073664]
63. Driver JP, Racine JJ, Ye C, Lamont DJ, Newby BN, Leeth CM, Chapman HD, Brusko TM, Chen YG, Mathews CE, and Serreze DV 2017 Interferon-γ limits diabetogenic CD8+T-cell effector responses in type 1 diabetes. Diabetes 66: 710–721. [PubMed: 27920091]
64. Cannons JL, Lu KT, and Schwartzberg PL 2013 T follicular helper cell diversity and plasticity. Trends Immunol. 34: 200–207. [PubMed: 23395212]
65. Kenefeck R, Wang CJ, Kapadi T, Wardzinski L, Attridge K, Clough LE, Heuts F, Kogimtzis A, Patel S, Rosenthal M, Ono M, Sansom DM, Narendran P, and Walker LSK 2015 Follicular helper T cell signature in type 1 diabetes. J. Clin. Invest 125: 292–303. [PubMed: 25485678]
66. Ferreira RC, Simons HZ, Thompson WS, Cutler AJ, Dopico XC, Smyth DJ, Mashar M, Schuilenburg H, Walker NM, Dunger DB, Wallace C, Todd JA, Wicker LS, and Pekalski ML 2015 IL-21 production by CD4+ effector T cells and frequency of circulating follicular helper T cells are increased in type 1 diabetes patients. Diabetologia 58: 781–790. [PubMed: 25652388]
67. Heninger AK, Eugster A, Kuehn D, Buettner F, Kuhn M, Lindner A, Dietz S, Jergens S, Wilhelm C, Beyerlein A, Ziegler AG, and Bonifacio E 2017 A divergent population of autoantigen-responsive CD4+ T cells in infants prior to b cell autoimmunity. Sci. Transl. Med 9: eaaf8848. [PubMed: 28228602]
68. Nakayamada S, Kanno Y, Takahashi H, Jankovic D, Lu KT, Johnson TA, wei Sun H, Vahedi G, Hakim O, Handon R, Schwartzberg PL, Hager GL, and O'Shea JJ 2011 Early Th1 Cell

Differentiation Is Marked by a Tfh Cell-like Transition. Immunity 35: 919–931. [PubMed: 22195747]

69. Hampe CS 2012 Protective role of anti-idiotypic antibodies in autoimmunity--lessons for type 1 diabetes. Autoimmunity 45: 320–331. [PubMed: 22288464]
70. Bonami RH, and Thomas JW 2015 Targeting Anti-Insulin B Cell Receptors Improves Receptor Editing in Type 1 Diabetes-Prone Mice. J. Immunol 195: 4730–4741. [PubMed: 26432895]
71. Tiller T, Meffre E, Yurasov S, Tsuiji M, Nussenzweig MC, and Wardemann H 2008 Efficient generation of monoclonal antibodies from single human B cells by single cell RT-PCR and expression vector cloning. J. Immunol. Methods 329: 112–124. [PubMed: 17996249]
72. Paun A, Yau C, and Danska JS 2017 The Influence of the Microbiome on Type 1 Diabetes. J. Immunol 198: 590–595. [PubMed: 28069754]
73. Mullaney JA, Stephens JE, Costello M-E, Fong C, Geeling BE, Gavin PG, Wright CM, Spector TD, Brown MA, and Hamilton-Williams EE 2018 Type 1 diabetes susceptibility alleles are associated with distinct alterations in the gut microbiota. Microbiome 6: 35–51. [PubMed: 29454391]

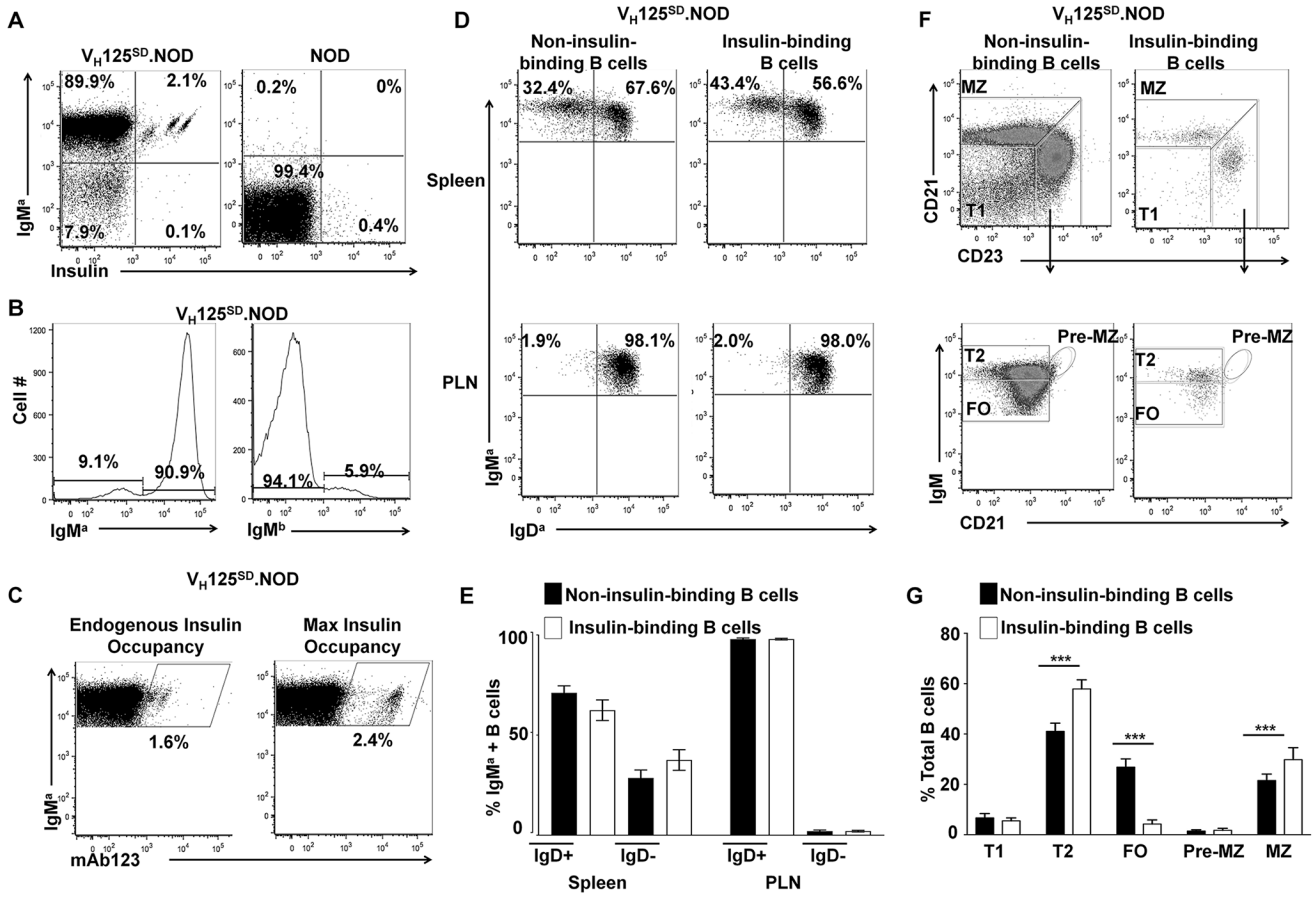

Fig. 1. Targeted anti-insulin VDJH (V_H125^{SD}.NOD) facilitates detection of anti-insulin B cells in NOD mice.

Lymphocytes from spleen and PLNs were isolated from V_H125^{SD}.NOD and non-transgenic NOD mice, and B cells (B220+CD19+) were analyzed by flow cytometry. (A) Representative dot plots showing IgM^a+ and insulin-binding on B cells from V_H125^{SD}.NOD mice (left) vs non-transgenic NOD mice (right). Anti-insulin B cells were identified using biotinylated human insulin and are located in the IgM^a+Insulin+ gate (upper right quadrants). Plots are representative of ≥ 14 mice for each genotype. (B) Flow cytometry staining for IgM^a (transgenic) and IgM^b (non-transgenic) B cells was used to assess allelic exclusion. Representative histograms of splenocytes from V_H125^{SD}.NOD mice are gated on B220+ live lymphocytes. (C) Flow cytometry using biotinylated mAb123 to detect insulin-occupied BCRs. B cells (B220+, IgM^a+) from V_H125^{SD}.NOD mice were stained with biotinylated mAb123 to detect endogenous insulin binding (left panel). B cells were incubated with insulin, washed, and then stained with biotinylated mAb123 to detect fully occupied BCRs (right panel). (D) Lymphocytes from spleen and PLNs were isolated from pre-diabetic, female, 8–12-week-old mice and flow cytometry was used to identify IgM^a and IgD^a expression in non-insulin-binding and insulin-binding B cells. Representative dot plots of IgM^a and IgD^a distribution are shown. (E) The mean percentage ± SD of IgM^a+ lymphocytes that were either IgD^a+ or IgD^a-, among non-insulin-binding (black), or insulin-binding (white) B cells, n≥3 mice. (F) B cell developmental subsets were identified in non-insulin-binding and insulin-binding B cell populations as follows: T1 ($CD21^{low}$ $CD23^{low}$

IgM^{high}), T2 (CD21^{low} CD23^{high} IgM^{high}), FO (CD21^{low} CD23^{high} IgM^{low}), Pre-MZ (CD21^{high} CD23^{high} IgM^{high}) and MZ (CD21^{high} CD23^{low} IgM^{high}). Plots are representative of ≥ 11 mice. (G) The mean percentage ± SD of each B cell subset is shown for non-insulin-binding (black) and insulin-binding (white) populations, *** $p < 0.001$, two-tailed t test.

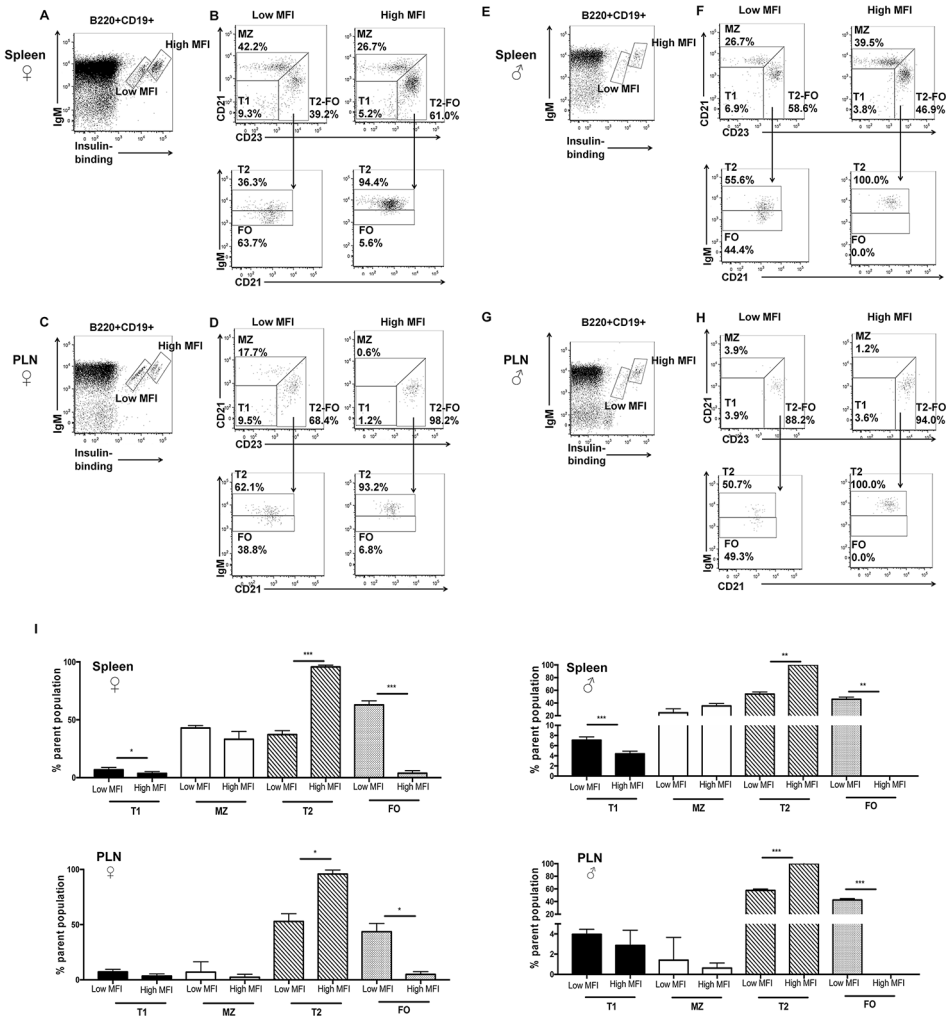

Fig. 2. Insulin-binding B cells are enriched in distinct subsets in V_H125^{SD}.NOD mice.

Cell suspensions from the spleen and PLNs of male and female, pre-diabetic, 8–12 week old mice were analyzed by flow cytometry. (A-G) Representative dot plots on B cells (B220+CD19+) from spleens and PLNs stained with IgM and biotinylated insulin to identify different populations of insulin-binding B cells (A, C, E, G) designated as “low MFI” and “high MFI” (boxes). (B, D, E, H) Flow-cytometry phenotyping on insulin-binding B cells residing in “low MFI” (left) and “high MFI” (right) populations. Upper plots identify T1, MZ and T2-FO subsets based on CD23 and CD21 staining. Lower plots (arrow) distinguish T2 and FO subsets using IgM and CD21 staining. Percentages reflect the percentage of the parent population. (I) Mean ± SD for percentages of B cell subsets for spleen and PLNs in male and female mice; n≥3 mice per group. *p<0.05, **p<0.01, ***p<0.001, paired, two-tailed t test.

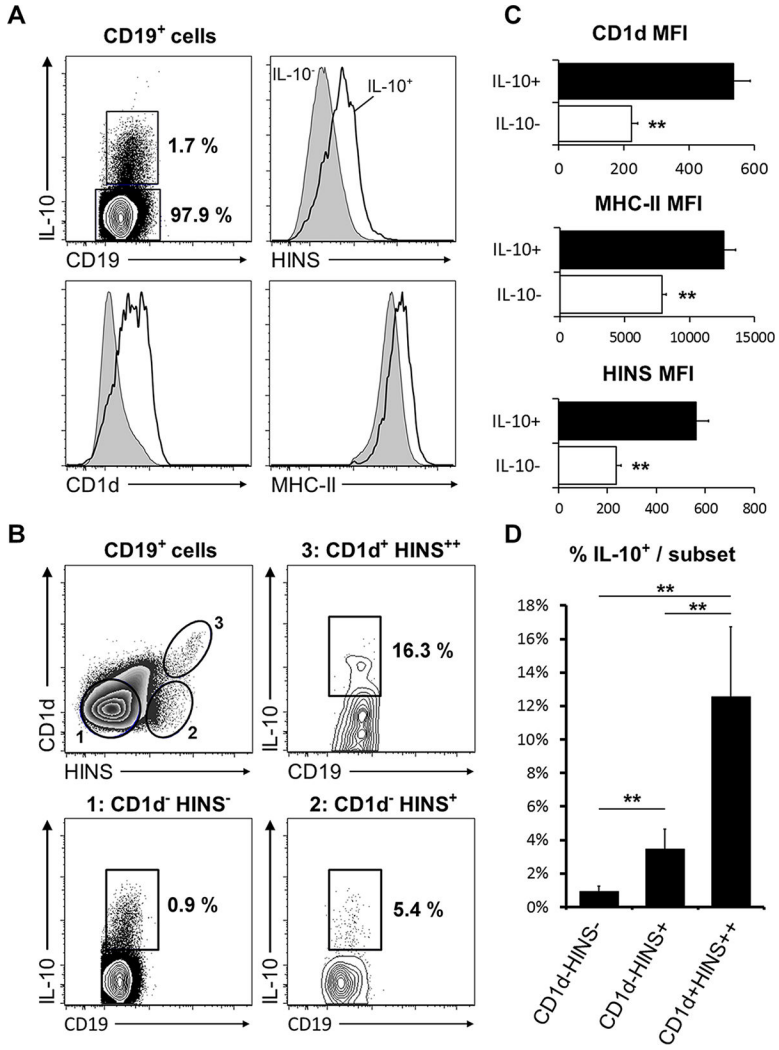

Fig. 3. Anti-insulin B cells have enhanced IL-10 production and express higher surface levels of antigen presentation molecules.

Splenic B cells from V_H125^{SD}.NOD mice (n=5 female, pre-diabetic mice, 12–16 weeks old) were assessed for IL-10 production capacity and surface expression of MHC-II, CD1d, and insulin-binding (HINS). (A) CD19+IL-10+ cells display increased surface levels of CD1d, MHC-II and insulin binding (HINS). (B) Summary of the MFI for CD1d, MHC-II and insulin binding (HINS) in IL-10- and IL-10+ B cells. (C) Representative gating of CD19+ cell surface expression of CD1d and HINS. Corresponding gates indicate IL-10 competence within each subset. (D) Summary of the percentages of CD19+IL-10+ cells within each subset. ** $p<0.01$, unpaired, heteroscedastic t-test.

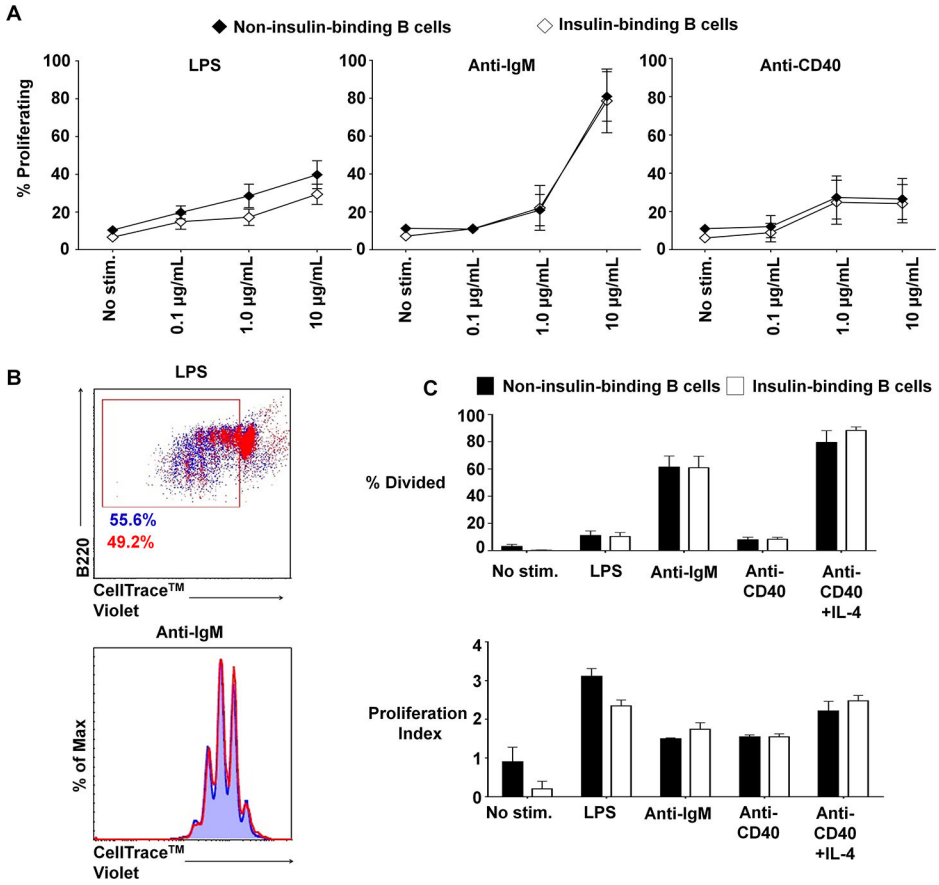

Fig. 4. Insulin-binding B cells in V_H125^{SD}.NOD mice proliferate normally in response to mitogens.

B cells purified from V_H125^{SD}.NOD mice were cultured with LPS, anti-IgM, or anti-CD40, and proliferation was assessed using CellTrace™ Violet labeling, gated on insulin-binding and non-insulin-binding B cells. (A) Dose responses to LPS, anti-IgM, and anti-CD40 were assessed for non-insulin-binding and insulin-binding using B cells purified from V_H125^{SD}.NOD mice. Mean response ± SEM is shown for each dose (n=5). (B, top panel) Representative dot plot illustrating proliferation in response to 10µg/ml LPS for non-insulin-binding B cells (blue) and insulin-binding B cells (red). Box designates proliferating cell populations. Cells were gated on B220+CD19+IgM^a+ live lymphocytes. (B, bottom panel) Representative histogram showing proliferation peaks for non-insulin-binding cells (blue tinted background and line) compared to insulin-binding cells (red line) after stimulation with 10µg/ml anti-IgM. Cells were gated on B220+CD19+ live lymphocytes. (C) Summary of proliferative responses as assessed by percentage of dividing cells (top panel) and proliferation index calculated using FlowJo v10.2 software (bottom panel) of B cells purified from V_H125^{SD}.NOD mice (n ≥3) and cultured for 3.5 days with media alone (no stimulation), LPS, anti-IgM, anti-CD40, or anti-CD40 + IL-4 as a positive control. Closed and open histograms denote non-insulin-binding and insulin-binding B cell populations, respectively. Error bars denote SEM.

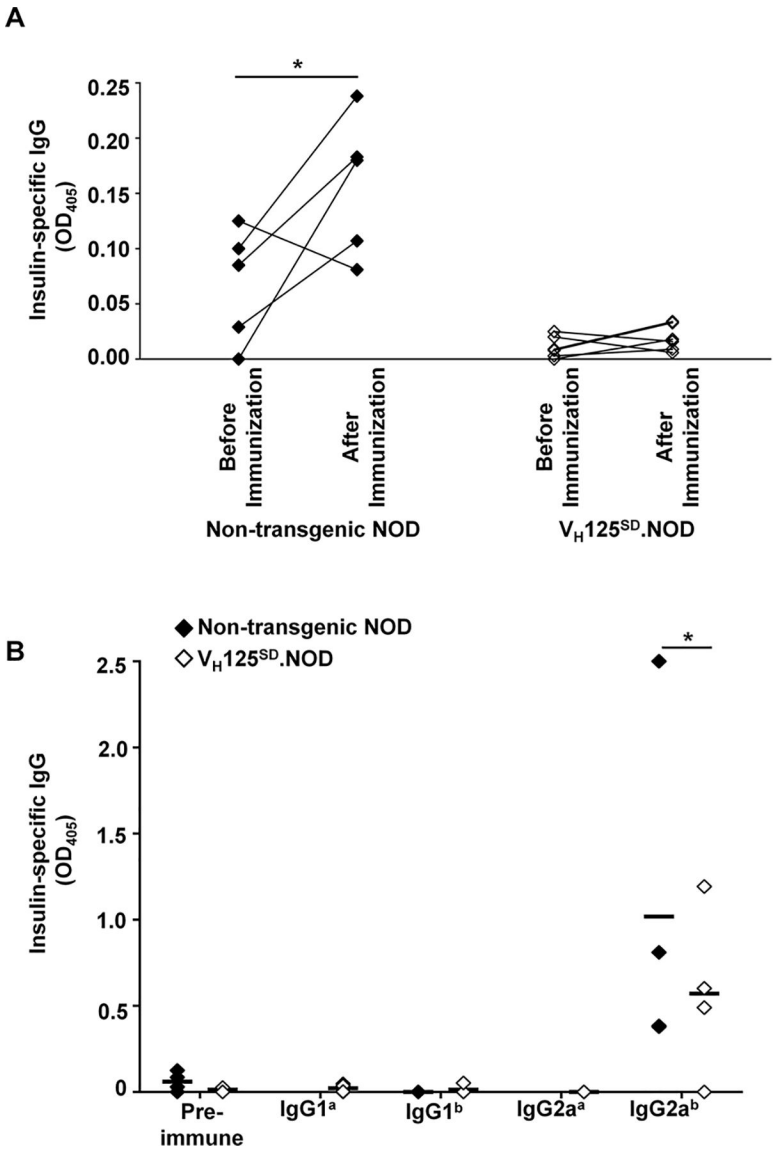

Fig. 5. Anti-insulin antibody production is impaired in V_H125^{SD}.NOD mice.

(A) Serum anti-insulin antibody production was measured by ELISA in non-transgenic NOD (n=5) and V_H125^{SD}.NOD (n=6) mice before and 2 weeks after immunization with insulin B:10–23 in CFA. All mice were male, pre-diabetic and 8–12 weeks of age. * $p < 0.05$, two-tailed t test. (B) Sera from non-transgenic NOD or V_H125^{SD}.NOD mice was harvested before immunization with B:10–23 in CFA (pre-immune) or 2 weeks following immunization. Insulin-specific antibody binding was measured by ELISA using secondary reagents for $IgG1^a$, $IgG1^b$, $IgG2a^a$ or $IgG2a^b$. Each symbol represents an individual mouse. Black bars represent mean, n≥3, * $p < 0.05$, Mann-Whitney test.

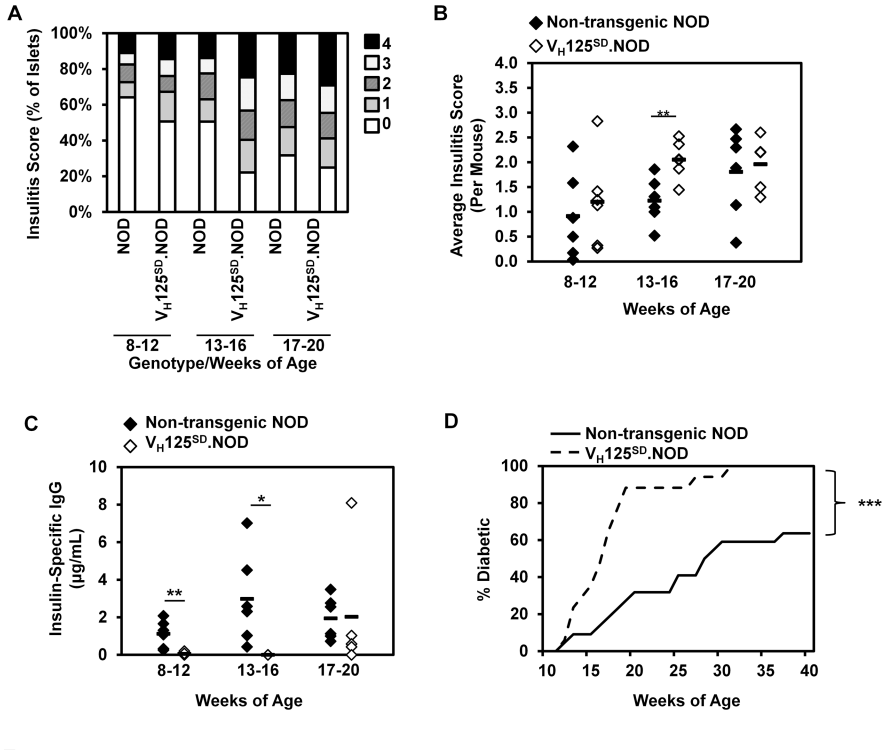

E

	Mean age at onset (weeks)			I-50%* (weeks)		
	Non-Tg	Tg	Δ (Tg -non-Tg)	Non-Tg	Tg	Δ (Tg -non-Tg)
Conventional (fixed IgM) VH125Tg.NOD						
Hulbert et al. (ref 16)	14	14	**0**	34	24	**10**
Kendall et al. (ref 34)	13	14	**1**	26	17	**9**
Henry et al. (ref 17)	12	10	**-2**	24	15	**9**
Class switch competent V_H125^{SD}.NOD						
Felton et al.	12	12	**0**	27	17	**10**
						***I-50% denotes >50% incidence**

Fig. 6. Anti-insulin VDJH125 targeted to the IgH locus accelerates insulitis and diabetes development in NOD mice.

(A) Summary of insulitis scores in pancreata histology from non-transgenic NOD and V_H125^{SD}.NOD mice. Female mice from the indicated age groups were used, n ≥ 5 mice per group. Scoring, described in Methods, ranges from 0 (no insulitis) to 4 (extensive invasion). (B) Average insulitis score per mouse is shown for non-transgenic NOD and V_H125^{SD}.NOD mice in the indicated age group, ** $p < 0.01$, two-tailed t test. (C) Spontaneous production of IgG autoantibodies to insulin in sera by ELISA from non-transgenic NOD (closed diamonds) or V_H125^{SD}.NOD mice (open diamonds) (n=18 per genotype, pre-diabetic, 8–20 weeks of age), * $p < 0.05$, ** $p < 0.01$, two-tailed t test. (D) Diabetes incidence curve in cohorts of female V_H125^{SD}.NOD mice (n= 13, solid line) compared to their non-transgenic littermates (n=13, dashed line). Mice were considered diabetic after the first of 2 consecutive blood glucoses were > 200mg/dl. *** $p < 0.001$ as calculated by a log-rank test. E) Table comparing mean age of diabetes onset and number of weeks at which diabetes incidence was > 50% (I-50%) in different cohorts of conventional (VH125Tg.NOD) and site-directed (V_H125^{SD}.NOD mice) and their littermate controls. Differences (Δ) in weeks between transgenic and control NOD mice are shown for each cohort.

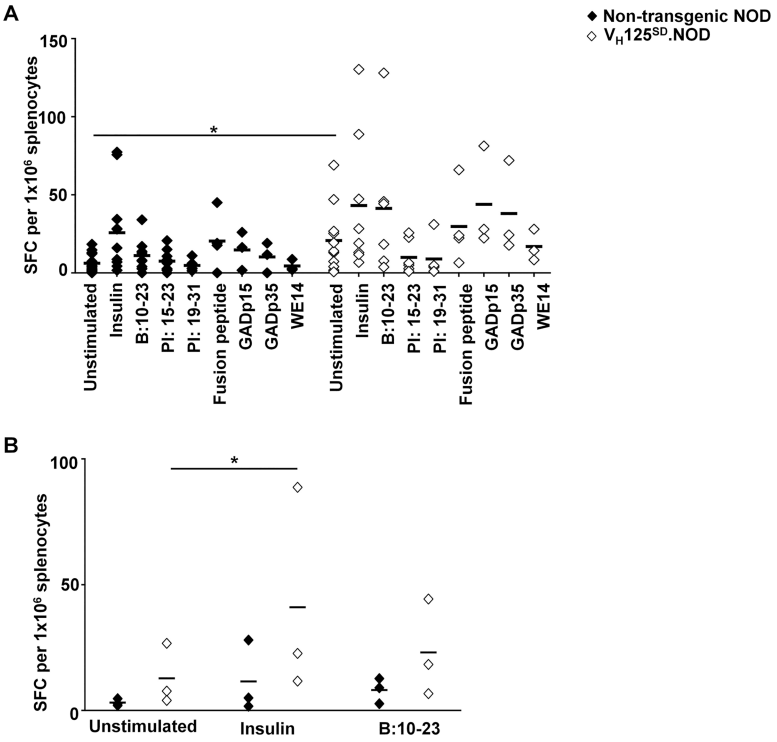

Fig. 7. T cell responses to a broad array of autoepitopes are increased in V$_H$125^{SD}.NOD mice.

(A) Splenocytes from female, pre-diabetic non-transgenic NOD (closed diamonds) or V$_H$125^{SD}.NOD mice (open diamonds) (n≥3 for each antigen) were cultured with the indicated insulin antigens (insulin and the immunodominant B chain peptide B:10–23), proinsulin peptides (PI: 15–23, mouse proinsulin-1; PI: 19–23, mouse proinsulin-2), or peptide epitopes from islet-associated autoantigens (HIP, fusion peptide; mouse GAD 217–236, GADp15, mouse GAD 524–534, GADp35; ChgA 342–355, WE14) for 72h and IFN-γ spot forming cells (SFCs) were quantified. Each point represents the mean number of IFN-γ SFCs for an individual mouse. A two-way ANOVA of antigen and genotype (V$_H$125^{SD}.NOD and non-transgenic NOD) on IFN-γ production was conducted, and a significant main effect of genotype on IFN-γ production was found, $F(1, 95) = 11.75$, $p<0.001$. (B) Splenocytes from age-matched female, pre-diabetic, non-transgenic NOD and their V$_H$125^{SD}.NOD littermates (n = 3 for each genotype) were cultured in the presence or absence of insulin or B:10–23 peptide for 72h. Response was assessed by quantifying number of IFN-γ SFCs. A two-way ANOVA of antigen and genotype (V$_H$125^{SD}.NOD and non-transgenic NOD) on IFN-γ production was conducted with Dunnett's multiple comparisons test, $F(1, 4) = 1.582$, $p=0.277$, *$p<0.05$.